Binary Tomography for Triplane Cardiography

Bruno M. Carvalho[1], Gabor T. Herman[1], Samuel Matej[1],
Claudia Salzberg[1], and Eilat Vardi[2]

[1] University of Pennsylvania, Department of Radiology, Medical Image Processing Group, Blockley Hall, Fourth Floor, 423 Guardian Drive, Philadelphia, PA 19104-6021, USA
{carvalho, gabor, matej, claudia}@mipg.upenn.edu
[2] Technion - Technical Institute of Israel, P.O. Box 41, Haifa 32000, Israel
seilat@techst02.technion.ac.il

Abstract. The problem of reconstructing a binary image (usually an image in the plane and not necessarily on a Cartesian grid) from a few projections translates into the problem of solving a system of equations which is very underdetermined and leads in general to a large class of solutions. It is desirable to limit the class of possible solutions, by using appropriate prior information, to only those which are reasonably typical of the class of images which contains the unknown image that we wish to reconstruct. One may indeed pose the following hypothesis: if the image is a typical member of a class of images having a certain distribution, then by using this information we can limit the class of possible solutions to only those which are close to the given unknown image. This hypothesis is experimentally validated for the specific case of a class of binary images representing cardiac cross-sections, where the probability of the occurrence of a particular image of the class is determined by a Gibbs distribution and reconstruction is to be done from the three noisy projections.

1 Introduction

The subject matter of this paper is the recovery of binary images from their projections. A binary image is a rectangular array of pixels, each one of which is either black or white. In the case of cardiac angiography, we can represent a section through the heart as a binary image in which white is assigned to those pixels which contain contrast material. A projection of a binary image is defined as a data set, which for every line (in a set of parallel lines, each of which goes through the center of every pixel which it intersects at all) tells us, at least approximately, how many white pixels are intersected by that line. According to this definition there can be only four projections: one horizontal, one vertical and two diagonal. There exist more general definitions of projections in the literature [1], but it is typical for many applications that only a few projections are available [2,3].

The problem of *binary tomography* is the recovery of a binary image from its projections. This problem can be represented by a system of equations which

A. Kuba et al. (Eds.): IPMI'99, LNCS 1613, pp. 29–41, 1999.

is very underdetermined and leads typically to a large class of solutions. It is desirable to reduce the class of possible solutions to only those which are reasonably "close" to the (unknown) image which gave rise to the measurement data. Appropriate prior information on the image may be useful for this task [4]. In addition to the inherent information in binary tomography that there are only two possible values, *Gibbs priors* [5,6] describing the local behavior/character of the image can also provide useful information. We pose the hypothesis that, for certain *Gibbs distributions*, knowledge that the image is a random element from the distribution is sufficient for limiting the class of possible solutions to only those which are close to the (unknown) image which gave rise to the measurement data.

Binary images can be described in many applications by the following simplified characterization: a set of *objects* - "white" regions - are located in a "black" background. (We adopt the convention that 1 represents white and 0 represents black.) This can be easily translated into Gibbs distributions by using a set of configurations of neighboring image elements and assigning a value (which is an indicator of the likelihood of occurrence) to each of these configurations.

One type of test presented in this paper is motivated by the task of reconstructing semiconductor surface layers from a few projections. Fishburn *et al.* [3] designed three test phantoms for assessing the suitability of binary tomography for that task. These phantoms have been recently used in the binary tomography literature by the several other researchers (see, e.g., [1]). The common experience reported by these researchers is that knowing the horizontal, vertical and one diagonal projection is not sufficient for exact recovery of such phantoms. However, it is shown in [7] that an algorithm, which makes use of an appropriate Gibbs prior, correctly recovers the test phantoms of [3] from three projections.

The following section introduces Gibbs distributions and discusses their definition using a look-up table. A reconstruction algorithm based on two given perfect projections and a Gibbs prior is presented in the third section, where it is also illustrated for the phantoms of [3] that the algorithm (while achieving its mathematical aim) fails to recover the original object. Since three projections are sufficient to recover these test phantoms based on semiconductor surface layers, it appears possible that three projections would also be sufficient for the recovery of cardiac cross-sections. An algorithm to do this is presented in Section 4; this algorithm does not assume that the projections are noiseless. Its performance is investigated in Section 5, where the influence of noise is also demonstrated. The final section presents our conclusions.

2 Gibbs Distributions Associated with Binary Images

Local properties of a given binary image ω defined on H pixels (each pixel is indexed by an integer h, $1 \leq h \leq H$, and $\omega(h)$ is either black or white) can be characterized by a Gibbs distribution of the form

$$\Pi(\omega) \;=\; \frac{1}{Z}\; e^{\beta \sum_{h=1}^{H} I_h(\omega)}\;, \tag{1}$$

where $\Pi(\omega)$ is the probability of occurrence of the image ω, Z is the normalizing factor (which insures that Π is a probability density function; i.e. that the sum of $\Pi(\omega)$ over all possible binary images is 1), β is a parameter defining the "peakedness" of the Gibbs distribution (this is one of the parameters controlling the appearance of the typical images), and $I_h(\omega)$ is the "local energy function" for the pixel indexed by h, $1 \leq h \leq H$. The local energy function is defined in such a way that it encourages certain local configurations, such as uniform white or black clusters of pixels and configurations forming edges or corners. Each of these configurations can be encouraged to a different extent by assigning to them a specific value. In this paper we have adopted the convention that the local energy function at a pixel depends only on its own color and those of its eight neighbors. Thus, the color of a particular pixel influences the value of the local energy function of only itself and its eight neighbors.

Appropriate definition of the local energy function plays an important role in successful image recovery. The definition should reflect the characteristics of a typical image of the particular application area. There are many possible ways of defining the local energy function. One of them is to use a look-up table which contains a value for each possible configuration. (In our case, there are 512 possible configurations.) Given an ensemble of typical images for a particular application (a training set), the look-up table can be created by counting the number of times each particular configuration appears in the images. Then the $I_h(\omega)$ of (1) is defined as $\ln(q+1)$, where q is the value in the look-up table of the local configuration in the image ω at the pixel h. The usefulness of the resulting prior depends on the size of the training set (the larger, the better) and on how representative the images in the training set are for the application area.

3 Biplane Tomography: Preliminary Experiments

Ryser showed in the 1950's [8] that if one matrix of 0's and 1's has the same row and column sums as another such matrix then the first matrix can be transformed into the second by a finite sequence of simple switching operations each of which changes two 1's to 0's and two 0's to 1's and leaves the row and column sums unaltered. This can be regarded as a result of binary tomography, since matrices of 0's and 1's can be viewed as binary images; two matrices that have the same row and column sums correspond to two binary images which have the same horizontal and vertical projections. We refer to such images as being *tomographically equivalent*. The simple switching operation described above will be referred to as a *rectangular 4-switch*.

Let $\mathcal{C}$ be any tomographic equivalence class of binary images. Consider the graph whose vertices are in $1-1$ correspondence with the binary images in $\mathcal{C}$, in which two vertices are adjacent if and only if the image corresponding to one vertex can be obtained from the image corresponding to the other by a single rectangular 4-switch. We will call this the *Ryser graph* of the tomographic equivalence class $\mathcal{C}$.

The Ryser graph is a finite graph since each tomographic equivalence class is finite. In view of Ryser's result [8], the Ryser graph is connected.

We now give an application of the Ryser graph. Let $\mathcal{P}$ be the set of all binary images. Consider the following problem: Given a binary image $\omega \in \mathcal{P}$, find an image in ω's tomographic equivalence class for which $\Pi(\omega)$ of (1) has a relatively high value. (Ideally, we would like to find an image that maximizes $\Pi(\omega)$, but we do not expect to always achieve this.)

Kong and Herman [9] describe (two versions of) an iterative stochastic algorithm to do this. The algorithm is a typical instance of a class of algorithms known in the literature as Metropolis algorithms [10]. Since such algorithms are often time consuming, [9] devotes a considerable amount of space to the achievement of a relatively efficient implementation. The essential idea is to first find a single binary image which satisfies the two given projections and then iteratively investigate the effect on $\Pi(\omega)$ of making a random rectangular 4-switch.

Roughly speaking, a single step in the Metropolis procedure starts with "randomly picking" a possible rectangular 4-switch for the current image ω_1. Let ω_2 be the image that is obtained by performing this rectangular 4-switch on ω_1. Let p be the ratio of $\Pi(\omega_2)$ to $\Pi(\omega_1)$. The single step of the iterative procedure is completed by replacing ω_1 by ω_2 if p is greater than 1, and replacing ω_1 by ω_2 with probability p (and hence retaining ω_1 with probability $1 - p$) if p is less than 1. As explained in [9], properties of Ryser graphs and of the Metropolis algorithms guarantee that the procedure just described will produce images ω with relatively high values of $\Pi(\omega)$; for a precise statement (as well as for a discussion of implementational concerns), see [9].

In order to test out our ideas on reconstructions from two projections, we implemented the algorithms described in [9] and applied them to the binary images in [3] representing semiconductor surface layers. (For these experiments, the lookup-table was created using the three phantoms of [3].) For all three phantoms (these are shown on the left of Figs. 1, 2 and 3, respectively), the algorithms of [9] performed "too well" in the sense that the reconstructed images (these are shown on the right of Figs. 1, 2 and 3, respectively) have a higher value of $\Pi(\omega)$ than the originals. One might say after looking at these figures that the reconstructions are versions of the original binary images in which the boundaries have been smoothed.

As a result of these preliminary experiments combined with the fact that all three phantoms of [3] were perfectly recovered when Gibbs priors were combined with three perfect projections [7], we decided to investigate the efficacy of triplane rather than biplane cardio-angiography.

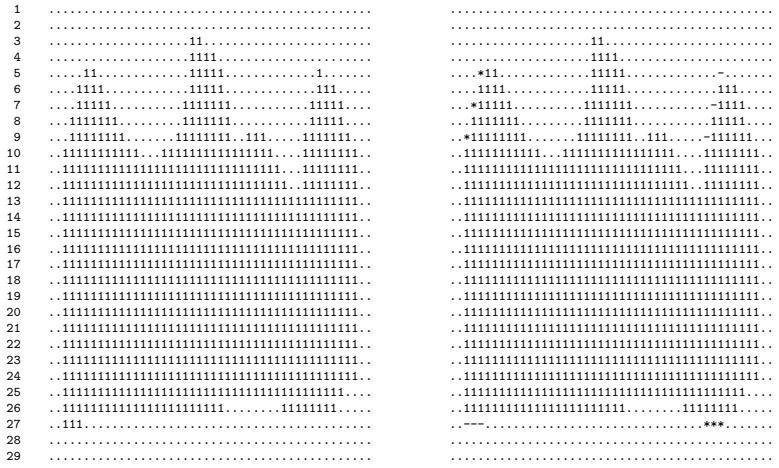

Fig. 1. Phantom 1 (left) and its reconstruction (right) based on Ryser graphs and a Metropolis algorithm from perfect horizontal and vertical projections; . and 1 represent the values zero and 1 (respectively) in the phantom and at correctly reconstructed locations; - and * represent incorrectly reconstructed values of zero and one (respectively); the total number of incorrectly reconstructed pixels is 12

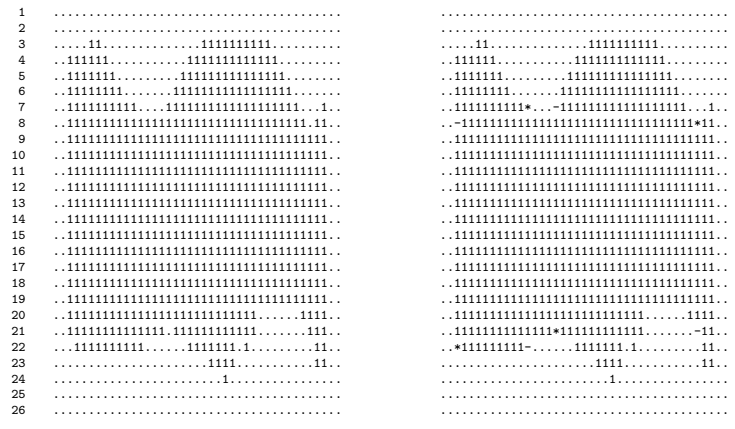

Fig. 2. Phantom 2 (left) and its reconstruction (right) based on Ryser graphs and a Metropolis algorithm from perfect horizontal and vertical projections; . and 1 represent the values zero and 1 (respectively) in the phantom and at correctly reconstructed locations; - and * represent incorrectly reconstructed values of zero and one (respectively); the total number of incorrectly reconstructed pixels is 8

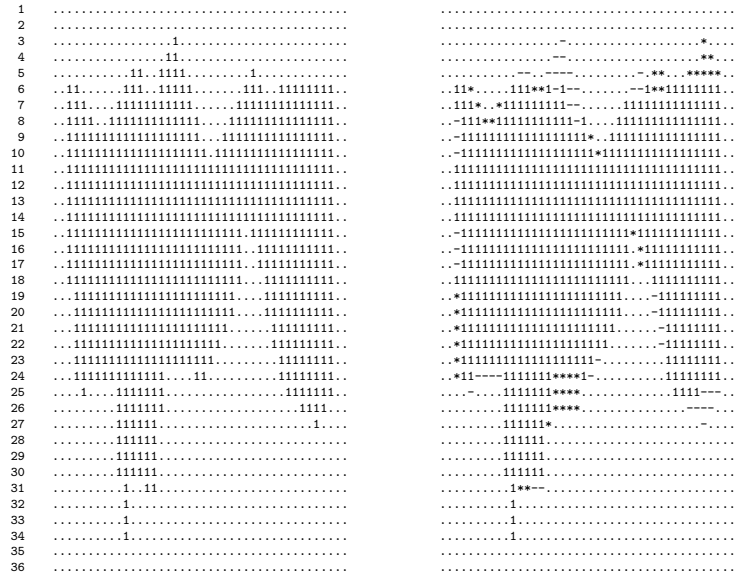

Fig. 3. Phantom 3 (left) and its reconstruction (right) based on Ryser graphs and a Metropolis algorithm from perfect horizontal and vertical projections; . and 1 represent the values zero and 1 (respectively) in the phantom and at correctly reconstructed locations; - and * represent incorrectly reconstructed values of zero and one (respectively); the total number of incorrectly reconstructed pixels is 90

4 A Reconstruction Algorithm for Three Noisy Projections

Assume that our data consist of estimates of three (horizontal, vertical and one diagonal) projections of an image, which we believe to be a random sample from a known Gibbs distribution. Then a reconstruction algorithm should find an image which is not only consistent with the data, but which is also a typical sample from the known Gibbs distribution. We use a modified Metropolis algorithm in which the search for a likely image is altered to take also into account the effect of replacing ω_1 by ω_2 on the consistency with the given projection data. Roughly speaking, if the data inconsistency is increased or decreased, then the change is discouraged or encouraged, respectively. The relative influence of the data inconsistency is controlled by a parameter α ($\alpha \geq 0$).

To be exact, the Metropolis algorithm is modified as follows. First, since it may no longer be possible to find a binary image which satisfies our (noisy) projection data exactly, we do not attempt to start the iterative process with such an image. (In the experiments which are reported below, the initial image is always totally black.) Second, in the iterative step, the current image ω_1 is

changed into ω_2 by randomly picking a single pixel h_1 and changing its color. The role of p is replaced by

$$p' = e^{\beta\left(\left\{\sum_{h\in N(h_1)}[I_h(\omega_2)-I_h(\omega_1)]\right\} - \alpha\left\{F_{h_1}(\omega_2)-F_{h_1}(\omega_1)\right\}\right)}, \tag{2}$$

where $N(h_1)$ is the set of at most nine pixels consisting of h_1 and its neighbors and

$$F_{h_1}(\omega) = |d_{h_1}(\omega) - m_{h_1}|, \tag{3}$$

$$d_{h_1}(\omega) = \sum_{i=1}^{3} d^i_{h_1}(\omega), \tag{4}$$

$$m_{h_1} = \sum_{i=1}^{3} m^i_{h_1}, \tag{5}$$

where $d^i_{h_1}(\omega)$ is the number of white pixels in image ω on the line going in the direction i through the pixel h_1 and $m^i_{h_1}$ is the value of the corresponding item in the given projection data. Finally, ω_2 may, or may not, replace ω_1 as determined by the Metropolis principle with p' defined as in (2). To be exact, ω_1 is replaced by ω_2 if p' is greater than 1 and ω_1 is replaced by ω_2 with probability p' (and hence ω_1 is retained with probability $1 - p'$) if p' is less than 1.

Such a procedure is guided preferentially towards images which have relatively large probability, as defined by (1), and are at the same time not too inconsistent with the projection data. The procedure is run for a "long time" (see below) and at its termination we select as its output that image from the sequence produced by it which has the maximum probability (1).

5 Triplane Tomography: Application to Cardiac Angiography

For this application, we have identified a statistical ensemble of mathematically described images based on cardiac cross-sectional images in [11]. These images all consisted of three geometrical objects (an ellipse representing the left ventricle, a circle representing the left atrium and the difference between two circular sectors representing the right ventricle) of statistically variable size, shape and location. By assigning white to every pixel whose center is inside one of these objects (and black to every other pixel) each mathematically described image gives rise to a binary image; we refer to such binary images as "phantoms". (The reason why the binary assumption is justified is that the intended application is *subtraction* angiography in which the projection data are obtained by subtracting a pre-injection x-ray picture from a post-injection x-ray picture; the difference is the

Fig. 4. Two of the 10 phantoms from the training set

projection data of the image containing either the injected contrast material or nothing.)

Ten phantoms were randomly generated to create our training set. (Two of these are shown in Fig. 4.) Based on them, we collected the Gibbs prior information, by simply counting the occurrences of each possible configuration of a 3×3 window over all the images of our training set. This produces a look-up table, and hence a Gibbs distribution, as explained in Section 2.

The phantoms were defined on the square grid with height and width equal to 63 pixels. Thus, in our experiments, we have H=3,969. The phantoms and the raysums were generated using the software SNARK93 [12] and the pixel size used was $1mm$, producing $63mm \times 63mm$ images. Using SNARK93, we added noise to the raysums generation, producing raysums corrupted by an additive noise of mean 0.0 and standard deviations (σ) equal to 0.0 (noiseless case), 0.5 and 1.0. Since SNARK93 generates the projection data based on the geometrically described objects, even the "noiseless" data are only approximations of the projections of binary images of the discretized phantoms.

In our experimental study we investigated the actual benefit of prior information for cardiac cross-sectional binary image reconstruction. Our testing set consisted of 10 phantoms (from the same ensemble as the training set, but statistically independent), and for each phantom and each noise level (0.0, 0.5 and 1.0) three projections were generated; horizontal ($\leftarrow$), vertical ($\downarrow$) and diagonal ($\swarrow$). Since the image size was 63×63, for each phantom and noise level we produced 63 horizontal, 63 vertical and 125 diagonal raysums, adding to a total of 251 raysums. The algorithm received as input the raysums generated by SNARK93 and values for α and β in (2). The values of α and β for the noiseless case were selected based on the Gibbs prior (look-up table), that was generated by scanning the images of the training set and counting the pixel configurations on a 3×3 window. Using this knowledge, we selected $\alpha = 23.0$ and $\beta = 0.1$ for the experiments using noiseless raysums. The selected α and β values balance

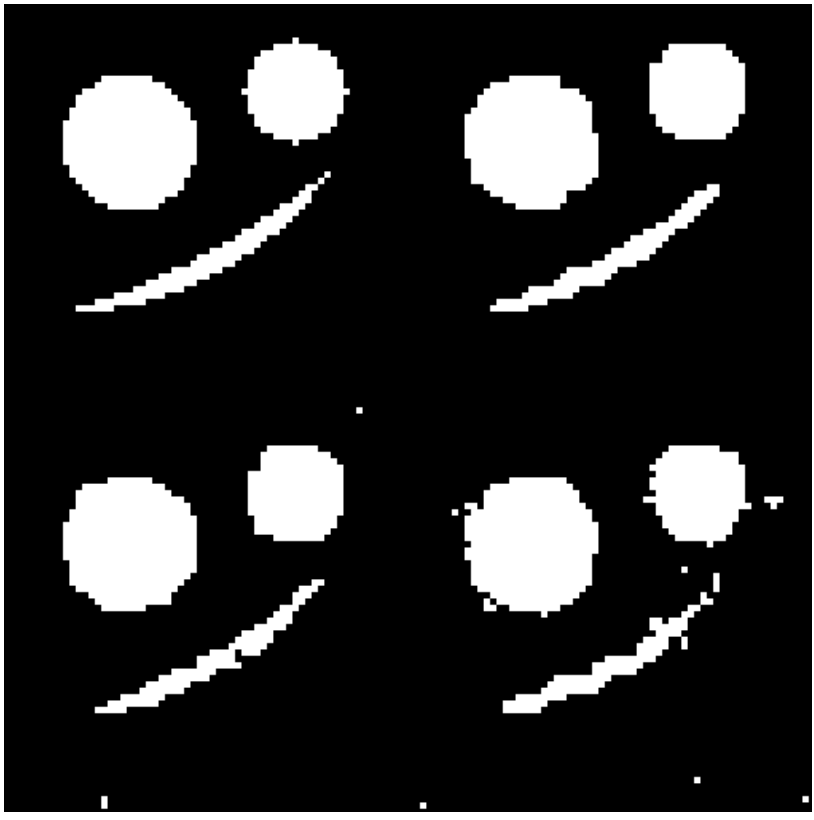

Fig. 5. A phantom (upper left corner) and its reconstructions using noiseless raysums (upper right corner) and raysums with additive noise of mean 0 and standard deviation (σ) of 0.5 (lower left corner) and 1.0 (lower right corner)

the contribution of the raysums and the Gibbs prior to the image reconstruction. Since, in the other cases, some noise was introduced into the raysums generation, we selected smaller α values, $\alpha = 18.4$ for $\sigma = 0.5$ and $\alpha = 13.8$ for $\sigma = 1.0$ (reflecting change in our confidence level on the raysums), while maintaining $\beta = 0.1$ for both cases.

For any binary image we define its *energy* as the sum of the local energy function over all pixels; i.e., $\sum_{h=1}^{H} I_h(w)$. In all experiments, the program outputs the image with the highest energy after 50,000 cycles (excluding the first 5,000 cycles, during which the totally black starting image could still have an influence on the image energy). In each cycle the algorithm randomly visits 3,969 pixels in the image and performs the modified Metropolis step as defined in Section 4. Using the phantom and the output image, we computed their energy difference, the number of pixels for which the output has a different color from the phantom and the total difference of their projections. Another quality measurement

Fig. 6. A phantom (upper left corner) and its reconstructions using noiseless raysums (upper right corner) and raysums with additive noise of mean 0 and standard deviation (σ) of 0.5 (lower left corner) and 1.0 (lower right corner)

used was the absolute difference (measured in pixels) of the areas of the objects representing the right ventricle, left ventricle and left atrium, in the phantom and in the reconstruction. In a reconstruction an "object" is defined as a component (a maximally connected subset) of the set of white pixels under 8-adjacency (two pixels are 8-adjacent if they share a corner or an edge). Two examples of a phantom (phantoms number 3 and 7) and the corresponding reconstructions using the raysums generated with the three different noise levels are shown in Figs. 5 and 6. (In this initial work we concentrated on investigating the possibility of accurate reconstructions from triplane data and paid no attention to the efficiency of implementation. Because of this the total computer time for the 50,000 cycles is 5 hours on an Sun ultra 10 300MHz.)

As can be seen in Table 1, all ten phantoms were reconstructed successfully for all three noise-levels. The table shows the results for the ten phantoms of the testing set with the three different noise levels for each one. The energy

Table 1. Table reporting the phantom numbers and energy values (Energy), and the energy difference (DEnr, where DEnr = $\text{Enr}_{phantom}$ - $\text{Enr}_{reconstruction}$), pixel difference (DPi) and projection difference (DPr) for reconstructions using raysums corrupted by three different noise levels ($\sigma = 0.0, 0.5$ and 1.0). The energy difference average is computed using the sum of the absolute values of the energy differences and all values in the last row (Avg) are calculated by averaging the ten individual values in the same column. (Negative values of DEnr indicate that the energy of the reconstruction is higher than that of the phantom)

Phantom		σ=0.0			σ=0.5			σ=1.0		
Num	Energy	DEnr	DPi	DPr	DEnr	DPi	DPr	DEnr	DPi	DPr
1	36480.53	-45.43	35	23	-11.40	54	42	596.05	98	82
2	36087.34	-50.89	60	24	-54.48	79	60	442.01	157	157
3	36986.62	-220.74	51	27	-27.03	60	61	662.92	105	106
4	37427.52	-77.94	72	23	-34.01	96	46	421.38	94	88
5	36344.12	-32.58	39	24	149.69	68	49	556.40	128	95
6	36171.59	16.10	44	26	148.82	80	55	682.61	127	84
7	36414.56	-30.55	41	31	32.81	61	40	751.89	141	97
8	36905.06	-97.57	49	24	-62.91	64	46	705.68	104	100
9	36273.46	-56.87	59	20	155.52	109	51	532.50	165	91
10	36064.98	-40.43	60	26	84.34	77	46	507.49	118	89
Avg	36515.58	-63.18	51	25	38.13	75	50	585.97	124	99

difference (DEnr) was computed as DEnr = $\text{Enr}_{phantom}$ - $\text{Enr}_{reconstruction}$, the pixel difference (DPi) reports the number of pixels that were different between the phantom and the reconstruction, and the projection difference (DPr) reports the sum of the absolute differences between the data (phantom raysums) and the projection sums for the reconstructed image. The total number of pixels and projections were equal to 3,969 and 251, respectively. The last row of Table 1 reports the average (Avg) of the absolute energy differences, pixel differences and projection differences for the ten phantoms. The averages pixel differences (DPi) and projection differences (DPr) were rounded to the nearest integer. The average percentages of misclassified pixels are 1.3% (if σ=0.0), 1.9% (if σ=0.5) and 3.1% (if σ=1.0).

The numbers reported for the phantoms in Table 2 refer to the total number of pixels in the three objects, while the numbers under LA, LV and RV report the absolute difference of the areas measured for the three objects in the phantom and reconstructions. The area difference averages (DA) reported in Table 2 contains information about all ten phantoms (rounded to the nearest integer). The average percentage errors in the areas are 1.0% (if σ=0.0), 1.3% (if σ=0.5) and 2.6% (if σ=1.0).

Since the choices of the α and β in (2) and the "measurement model" expressed in (3)-(5) are somewhat arbitrary, we have looked into the possibility of improving on our results by a more careful choice of these. To date we have not

Table 2. Table reporting the areas for the three objects (left atrium, left ventricle and right ventricle) in the phantoms and the absolute difference between the the object areas in the phantom and in the reconstructions using raysums corrupted by three different noise levels ($\sigma = 0.0, 0.5$ and 1.0). The last row reports the average of such differences (DA) for each object over all phantoms rounded to the nearest integer

Phantom				σ=0.0			σ=0.5			σ=1.0		
Num	LA	LV	RV	LA	LV	RV	LA	LV	RV	LA	LV	RV
1	293	441	170	0	1	8	0	2	4	11	8	3
2	213	539	238	7	1	1	7	3	4	8	2	16
3	197	355	119	0	1	0	2	5	8	5	9	11
4	109	439	101	2	2	1	1	2	0	2	3	11
5	97	527	358	3	4	2	3	1	4	7	3	2
6	177	469	382	1	1	2	3	10	3	10	3	4
7	177	389	367	2	7	2	5	2	0	5	1	2
8	177	349	255	10	1	1	8	2	3	18	7	3
9	185	583	218	1	2	0	4	5	12	1	5	15
10	225	515	349	3	2	3	0	1	0	2	11	7
DA	182	452	258	3	2	2	3	3	4	7	5	7

succeeded to do this; other models we tried did not improve upon the results resported in Tables 1 and 2.

6 Conclusions

We have shown how Gibbs priors can be defined and used in binary reconstruction problems. Experimental tests were done for the case when data are known for two or three projections. An algorithm based on the Ryser graph and the Metropolis algorithm was tested and it was found that two views were not sufficient to determine the object even if the data are noiseless and the Gibbs prior is based on the very pictures to be reconstructed. On the other hand, in the case of three views, our results indicate that a similar approach could be useful in triplane cardiac angiography even in the presence of noise in the data.

A modified Metropolis algorithm based on the known Gibbs prior proved to provide a good tool to move the reconstruction process towards the correct solution when the projection data by themselves are not sufficient to find such a solution. Our experiments suggest that if an algorithm is able to maximize the Gibbs probability subject to consistency with the data, then it is likely to be able to (nearly) recover a random image from the Gibbs distribution. This supports our hypothesis posed in the introduction, namely that if an image is a typical member of a class of images having a certain Gibbs distribution, then by using this information we can usually limit the class of possible solutions to only those which are close to the (unknown) image which gave rise to the measurement data.

Acknowledgements

This work was supported by the National Science Foundation Grant DMS-9612077, by the National Institutes of Health Grants HL-28438 and CA-54356 and by CAPES-BRASILIA-BRAZIL.

References

1. Herman, G.T., Kuba, A. (eds.): Special Issue on Discrete Tomography. Int. J. Imaging Syst. and Technol. **9** No. 2/3 (1998)
2. Chang, S.-K., Chow, C. K.: The Reconstruction of Three-Dimensional Objects from Two Orthogonal Projections and its Application to Cardiac Cineangiography. IEEE Trans. on Computers **22** (1973) 18-28
3. Fishburn, P., Schwander, P., Shepp, L., Vanderbei, R.J.: The Discrete Radon Transform and its Approximate Inversion via Linear Programming. Discrete Applied Mathematics **75** (1997) 39-61
4. Chan, M.T., Herman, G.T., Levitan, E.: A Bayesian Approach to PET Reconstruction Using Image-Modeling Gibbs Priors: Implementation and Comparison. IEEE Trans. Nucl. Sci. **44** (1997) 1347-1354
5. Winkler, G.: Image Analysis, Random Fields and Dynamic Monte Carlo Methods. Springer-Verlag, Berlin Heidelberg New York (1995)
6. Levitan, E., Chan, M., Herman, G.T.: Image-Modeling Gibbs Priors. Graph. Models Image Proc. **57** (1995) 117-130
7. Matej, S., Vardi, A., Herman, G.T., Vardi, E.: Binary Tomography Using Gibbs Priors. In Herman, G.T., Kuba, A. (eds.): Discrete Tomography: Foundations, Algorithms and Applications. Birkhauser, Boston Cambridge (to appear)
8. Ryser, H.J.: Combinatorial Properties of Matrices of Zeros and Ones. Can. J. Mathematics **9** (1957) 371-377
9. Kong, T.Y., Herman, G.T.: Tomographic Equivalence and Switching Operations. In Herman, G.T., Kuba, A. (eds.): Discrete Tomography: Foundations, Algorithms and Applications. Birkhauser, Boston Cambridge (to appear)
10. Metropolis, N., Rosenbluth, A.W., Rosenbluth, M.N., Teller, A.H., Teller, E.: Equations of State Calculations by Fast Computing Machines. J. Chem. Phys. **21**, (1953) 1087-1092
11. Ritman, E.L., Robb, R.A., Harris, L.D.: Imaging Physiological Functions. Praeger, New York (1985)
12. Browne, J.A., Herman, G.T., Odhner, D.: SNARK93: A Programming System for Image Reconstruction from Projections. Technical Report No. **198**. Medical Image Processing Group, Department of Radiology, University of Pennsylvania, Philadelphia (1993)